ELSEVIER

Journal of Power Sources 75 (1998) 64–72

JOURNAL OF POWER SOURCES

Coke vs. graphite as anodes for lithium-ion batteries

Hang Shi *

Valence Technology, 301 Conestoga Way, Henderson, NV 89015, USA

Received 26 January 1998; accepted 30 March 1998

Abstract

The respective rapid charge capabilities for graphite and coke for use in lithium-ion electrochemical cells were investigated. Lithium-ion cells with graphite anodes showed a poor ability to be rapidly charged due to the nature of the lithium intercalation process associated with graphite. By contrast, lithium-ion cells with coke anodes showed a much better quick-charge capability compared to that of graphite cells. In this paper, a series of experiments was carried out in order to characterize the difference in quick-charge capability between graphite and coke anode cells. Lithium manganese oxide was used as the cathode material. A mathematical simulation model developed by Newman and Doyle [J. Newman and M. Doyle, J. Electrochem. Soc. 143 (1996) 1890.] was also used in order to explore the change of lithium distribution in the anode as the cells were charged and discharged. The simulation results supported the experimental observation that coke has a superior ability to quickly distribute the lithium into the anode during high-rate charging.

Keywords: Cathode/anode ratio; Lithium insertion; Lithium-ion cells

1. Introduction

Research into higher energy and power densities in rechargeable batteries has intensified worldwide due to the continued increase in the demand for greater portable power, especially due to portable electronics and the advent of electric vehicles (EV). Existing battery technologies cannot satisfy the requirements of many advanced and emerging technologies, both in energy and power densities. Lithium-ion batteries, which utilize two different lithium intercalation compounds as their cathode and anode materials to store lithium during the charge and discharge cycles, have impacted the entire rechargeable battery industry significantly. Since the introduction of commercially available lithium-ion batteries by Sony in 1990 [1], the potential performance of this technology has quickly attracted worldwide battery research interest. Today, lithium-ion batteries are considered the most likely system to meet both energy and power densities for present and emerging technology applications.

Carbons (amorphous coke and crystalline graphite) and lithiated metal oxides (e.g., $LiMn_2O_4$, $LiCoO_2$ and $LiNiO_2$, etc.) are the most commonly used anode and cathode materials, respectively, in commercially available lithium-ion cells. Although historically amorphous carbons were first used in commercial lithium-ion batteries [1], graphites have eclipsed the use of amorphous carbons as anode active materials in most commercial production [2]. Graphite is favored primarily due to its high lithium intercalation capacity (up to 372 mA h/g) and its low, flat lithium intercalation voltage curve. The low and flat lithium intercalation potential of graphite ($\sim$ 100 mV vs. Li) is a desirable factor for the maintenance of a flat cell voltage output, and to maximize the cell's energy density. In contrast, the reversible capacities of a typical commercial coke material (about 160–220 mA h/g, depending upon the specific coke material) are significantly lower than that for graphite. Furthermore, amorphous carbon materials usually have a sloping lithium insertion voltage between 0 and 1 V. However, coke-type materials do have advantages over crystalline graphites in some aspects. One example is the flexibility of selecting compatible organic electrolytes for the coke anode. Propylene carbonate (PC) exhibits many attractive properties as an electrolyte solvent for lithium-ion batteries when compared to ethylene carbonate (EC) or dimethyl carbonate (DMC) solvents, such as a higher salt solubility, lower melting temperature, high boiling point, and lower toxicity. Some PC-based electrolytes have a proven stability and excellent performance

* E-mail: hangshi@yahoo.com

0378-7753/98/$19.00
PII S0378-7753(98)00093-7

at both high and low temperatures, which is one of the most desired characteristics for battery applications. Unfortunately, most graphite anodes have a compatibility problem with PC-based electrolytes, due to strong electrochemical reaction between the graphite surface and the PC solvent. Such a reaction causes the solvent molecules to co-intercalate into graphite and normally results in an unacceptably high first-cycle loss [3]. On the other hand, coke [1] works well with most PC-based electrolytes because of its different surface morphology and structure. In the past decade, considerable work has been performed to understand the different mechanisms of lithium insertion as they occur in various carbon materials [4]. Although some properties of lithium insertion in carbons are still poorly understood, it is clear that both graphite and coke have advantages and disadvantages for use as anodes. The specific product application is the key in determining whether graphite or coke should be used in a given battery system.

In certain applications, such as electric vehicles (EV), quick-charge capability (say, 2–3 C rate) is a requirement for the battery system. Fundamentally, the quick-charge capability of a lithium-ion cell is governed by the anode material, graphite or coke. During the charge cycle of a lithium-ion cell, lithium ions are dissociated from the cathode material dissolved into the electrolyte, and then inserted into the carbon anode. For most lithium intercalation compounds, the electrochemical lithium deinsertion process is more rapid than that of electrochemical lithium insertion. This can be understood from the general thermodynamic rule of order–disorder transitions. The lithium deinsertion process is equivalent to an order-to-disorder phase transition process, i.e., the ordered lithium ions undergo a change from an ordered phase in the cathode or anode (in graphite's case, an ordered staging phase) to a disordered phase in the electrolyte. The opposite process, lithium intercalation, is a disorder-to-order phase transition, i.e., the lithium ions undergo a change from a disordered phase in the electrolyte into an ordered phase in the cathode or anode. From thermodynamics, the order-to-disorder transition is a favored process (an increase in entropy), compared to the disorder-to-order transition (a decrease in entropy). Therefore, the selection of an appropriate carbon is critical in order to improve the charge rate capability of lithium-ion batteries.

The differences between graphite and coke can be characterized by several methods. Structurally, graphite is a crystalline material and coke is an amorphous material. Fig. 1 compares the X-ray diffraction (XRD) patterns of typical graphite and coke materials. The sharp peaks in the graphite X-ray profile and the broad peaks in the coke XRD profile indicate the crystalline structure of graphite

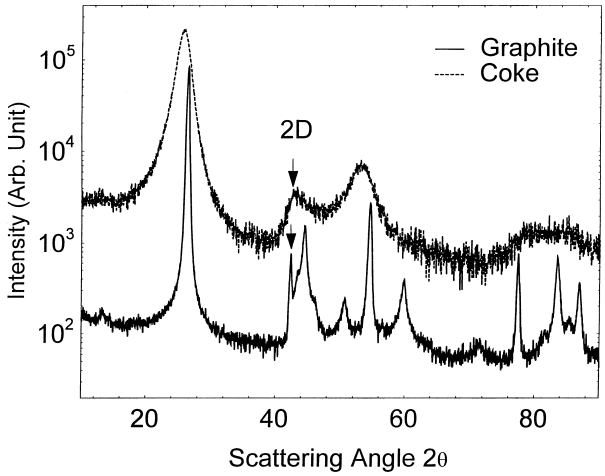

Fig. 1. XRD patterns for graphite and coke material used in this work. The coke pattern was shifted by an arbitrary unit for clarity. The broad peaks in the coke's pattern indicate its amorphous structure. The peaks identified with the small arrows are contributed from two-dimensional carbon layers in the coke or graphite material. The broader the peaks, the smaller the carbon layers in the material. The figure shows that coke has much smaller carbon layers than graphite.

and the amorphous structure of coke. Furthermore, according to the Scherrer equation [5,7]

$$L_a = 1.84\lambda / B\cos\theta, \quad (1)$$

where L_a is the dimension of the carbon layer, B is the angular width of the 2D diffraction peak at half-maximum intensity and θ is the Bragg angle. The equation shows that the broader the 2D peak, the smaller the carbon layers. The 2D peak sharpness of coke and graphite (shown in Fig. 1 with an arrow) indicates that the size of the carbon layer in the coke is much smaller than that of the graphite. The average size of the carbon layers (L_a) is 10–20 Å for coke and 500–1000 Å for graphite. The inherently smaller carbon layers of coke can significantly accelerate the solid ionic diffusion process and, therefore, results in a faster lithium insertion reaction than that for graphite. Electrochemically, graphite and coke also behave quite differently. Fig. 2 shows the voltage curves of the first discharge and charge (vs. lithium) for both graphite and coke. The data were collected using the electrochemical voltage spectroscopy (EVS) method [6], at about a 50-h rate. The lithium insertion voltage in the coke material is much higher and more sloped than that for the graphite. This high potential gradient and high average voltage vs. Li/Li^+ couple in coke will result in a much stronger driving force for lithium migration during the lithium insertion reaction when compared to the flattened and low insertion potential in the graphite material, and also prevents the coke anode from being plated by lithium during high-rate charging. The sloping coke voltage is, therefore, more favorable for quick lithium insertion and deinsertion during high-rate cell operation [8]. Considering the factors discussed above, one should expect the coke anode to outperform a graphite

[1] The word coke will be used interchangeably in the rest of the text to mean all amorphous carbon and cokes.

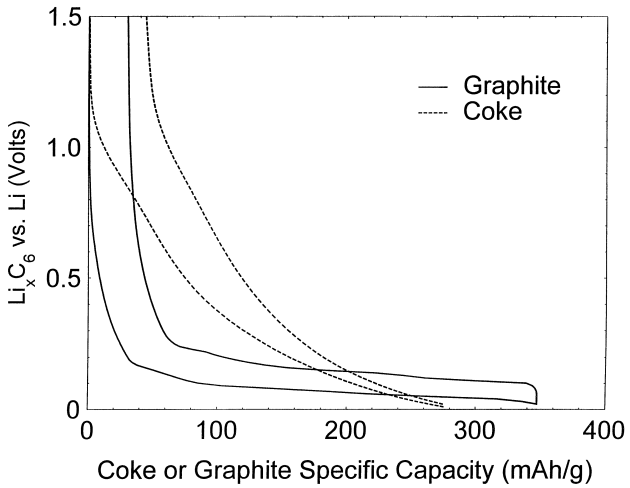

Fig. 2. Lithium insertion voltage profiles of graphite and coke material used in this work. Data were collected using a carbon/lithium foil half cell with EC:DMC (2:1 w/w) and $LiPF_6$ lithium salt. The electrochemical measurement was done by slow rate scan (EVS). A typical low and flat voltage profile for graphite and a sloping voltage profile for coke are shown.

anode under quick-charge conditions. In this paper, a series of comparative studies of rapid lithium insertion into coke and graphite anodes is performed and discussed.

2. Experimental

In all test cells used for this study, commercially available graphite and coke materials were used as anode active materials and a lithiated manganese oxide (LMO), also obtained from a commercial source, was used as the cathode active material. Test cells were of the Bellcore-type polymer lithium-ion cell (PLiON™) [9]. All cells have the usual lithium-ion configuration:

anode (graphite, coke)|separator|cathode (LMO).

The fabrication methods for this type of cell have been published and can be found in Ref. [9]. Both electrodes and the separator/electrolyte are based on the same plasticized fluoropolymer binder, a copolymer of vinylidene fluoride and hexafluoropropylene (P(VDF–HFP)). Each porous electrode consists of a homogeneous mixture of the active insertion materials (lithiated manganese oxide for cathode and graphite/coke for anode), the polymer matrix, a non-aqueous liquid electrolyte (EC:DMC (2:1 w/w) with $LiPF_6$), and a conductive filler additive. The expanded metal current collectors were either aluminum (for the positive electrode) or copper (for the negative electrode). The test cell had a geometric surface area of 24 cm^2 for both the anode and the cathode.

The specific capacities for the graphite and coke used in this work, measured using electrochemical voltage spectroscopy (EVS) [6], were 340 mA h/g and 215 mA h/g, respectively. In practical cells, the utilization of graphite and coke in anodes was less than these values, and dependent on the cathode/anode ratio, as well as on the current density. In order to determine the influence of carbon utilization on rate capability, test cells with different levels of anode utilization were constructed by carefully controlling the cathode/anode ratio (R),

$$R = \text{Mass of LMO in cathode/Mass of Carbon in anode.} \quad (2)$$

The cathode/anode ratio (R) controls the actual carbon utilization in the anode because of the cathode's limiting characteristics on the cell. The higher the R value in a cell, the higher the carbon utilization of the anode. In this work, three cell groups with different R values for graphite and two cell groups with different R values for coke were built in order to study the relation between cell-rate capability and carbon utilization. Table 1 summarizes the different groups of cells, their corresponding R values and typical carbon utilizations (based on an approximate C/4 rate). The cells with the highest R value assembled in this work were graphite cells in the G3 group ($R = 3.0$) and coke cells in the C2 group ($R = 2.5$), respectively. Under these ratios, the anode was almost fully utilized. For lower anode utilization, the graphite cells in group G2 ($R = 2.5$) and coke cells in group C1 ($R = 2.0$) were used throughout this study as the baseline values for comparative investigation. The graphite cells in group G1 ($R = 2.0$) and coke cells in group C2 ($R = 2.5$) utilized similar specific capacities from their carbon anode. These two cell groups were also compared for their rate capability independent of the cell's capacity utilization.

The rate capabilities of cells were tested by charge–discharge cycling between 3.0 V and 4.2 V. A constant-voltage float was used immediately after the cell reached the upper voltage limit of 4.2 V. The cut-off criteria for the constant voltage float was when the float current dropped to 10% of the original value. At normally used charge rates, the voltage float was required to fully charge the cell due to the sluggish lithium insertion kinetics of the carbon

Table 1
Summary of cathode/anode ratios (R) and carbon utilization in anodes for three groups of graphite cells and two groups of coke cells studied in this work (C/4 rate)

Test cells	Cell I.D.	Ratio of cathode/anode	Anode utilization (mA h/g)
Graphite / LMO (EVS: 340 mA h / g)	G1	2.0	206
	G2	2.5	260
	G3	3.0	312
Coke / LMO (EVS: 215 mA h / g)	C1	2.0	170
	C2	2.5	205

The low rate (EVS) specific capacities for the graphite and coke used in this work are also indicated.

anode. There was also a 10-min post-charge rest and a 30-min post-discharge rest in each cycle. Fig. 3 shows the voltage and current profiles for the second charge and discharge cycle at a C/2 rate for a graphite cell in group G2 ($R = 2.5$). The charge capacity contributed by the voltage floating was not a negligible portion when compared to that from constant current charging. The voltage float, however, also increases the total charge time due to the decreasing charge current during the float. To quantify the cell's quick-charge capability, the ratio of the charge time (T_c) to the discharge time (T_d) (Fig. 3) was used in this work.

$$P = T_c/T_d \quad (3)$$

The larger the P value, the worse the quick-charge capability of a cell. The data shown in Fig. 3 have a P value equal to 1.29. In the ideal case, a cell will have an unlimited charge capability, thus, no float current would be needed to charge the cell. The charge time would therefore be equal to the discharge time ($P = 1$). For actual cells, P is always larger than unity and is strongly dependent on charge rate and method of cell construction. The higher the charge rate, the longer a voltage float is needed, and consequently, the larger the P value for the cell. The cell construction and the cell chemistry also have a strong influence on the P value. Fig. 4 shows that, for the same charge rate as that used in Fig. 3, the coke anode cell ($R = 2.0$) required a much shorter charge float time. The P value was 1.16, much less than that for Fig. 3. In other words, the coke anode exhibited a better rate capability than that of the graphite anode. In this paper, one examines the factors which most significantly influence the quick-charge capability of carbon anode-based lithium-ion cells. The dependence of the P value on various factors such as carbon material, charge rate, cycle life, environment temperature are presented. In order to better understand the differences between lithium insertion behaviors in graphite and coke anodes, a mathematical simulation model developed by Newman and Doyle for lithium-ion cells has also been applied in the exploration of the lithium distribution patterns in the cell's anode during charging and discharging [10]. The simulation results are consistent with the experimental data which shows that coke is an intrinsically better material for lithium-ion batteries in terms of quick-charge capability.

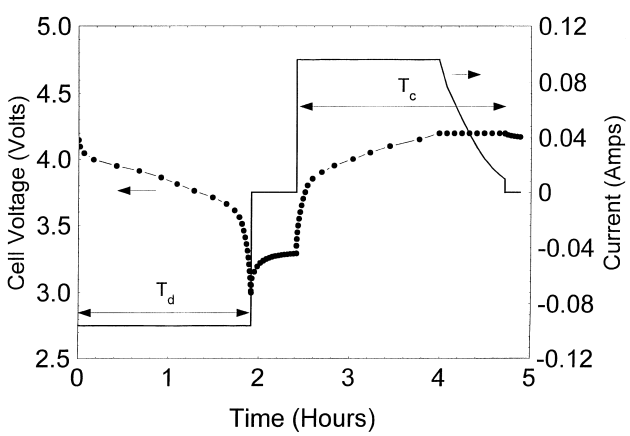

Fig. 3. Typical voltage and current profiles of a graphite anode cell (in group G2) collected in the second cycle by charging and discharging the cell between 3.0 V and 4.2 V at an approximate C/2 rate. The voltage float is clearly shown in the decreasing current tail. The charge time T_c and discharge time T_d are also indicated.

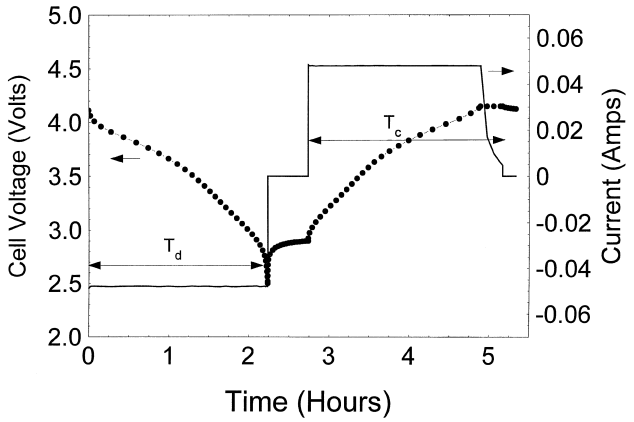

Fig. 4. Typical voltage and current profiles of a coke anode cell (in group C1) collected in the second cycle by charging and discharging the cell between 2.5 V and 4.15 V at an approximate C/2 rate. The constant voltage float can be seen in the current profile.

3. Results and discussions

Fig. 5 shows a series of the second-cycle voltage and current profiles for the four graphite anode cells in group G2 at various charge rates from 0.23 C up to 1.12 C. The charge rates were calculated based on the second discharge capacity of the cells. It can be seen that as rates gradually

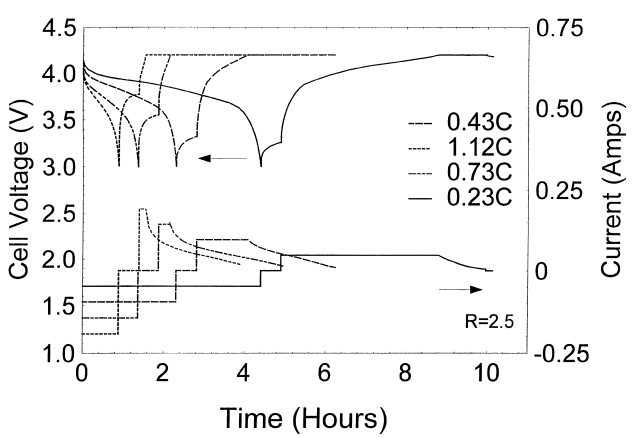

Fig. 5. Four voltage and current profiles collected at the second cycle from four graphite cells in group G2. Each cell was discharged and charged at a different current rate ranging from 0.23 C up to 1.12 C. As charge rate increased, the charge time becomes longer, and therefore, the P values for each rate increased dramatically from 1.19 to 2.81.

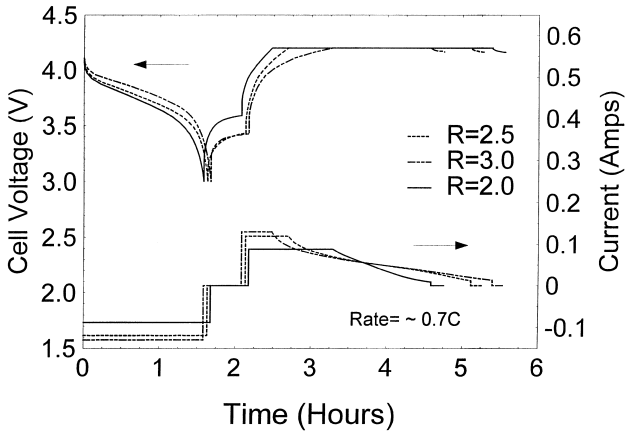

Fig. 6. Three voltage and current profiles collected on the second cycle for one graphite cell selected from each of the three graphite groups G1, G2 and G3. Each cell has a different cathode/anode ratio and was discharged and charged at the same current rate, approximately 0.7 C. It can be seen that as the cathode/anode ratio increases from 2.0 to 3.0, the current float time during charge correspondingly increases.

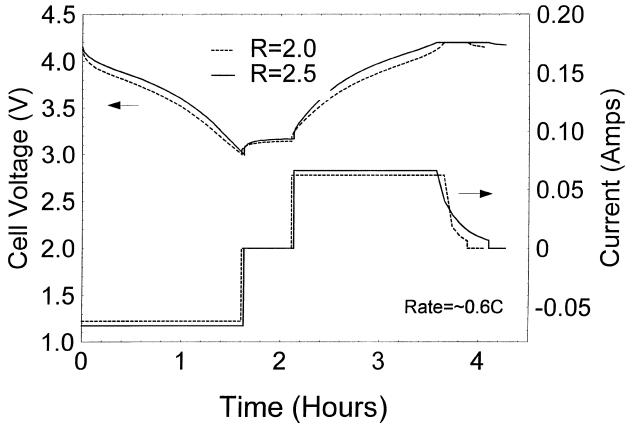

Fig. 8. Two voltage and current profiles collected on the second cycle of two coke cells selected from group cells C1 and C2. Each cell has a different cathode/anode ratio (R) and was discharged and charged at the same current rate, approximately 0.6 C. For the cell with the higher cathode/anode ratio, the increase in the current float time was much less dramatic than that for the graphite cells.

increased, the charge float times for charge current profiles, shown in Fig. 5, also increased. The P value increased dramatically from 1.19 for 0.23 C to 2.81 for 1.12 C. The R value also had a significant effect on the P value. Fig. 6 shows the voltage and current profiles for three graphite cells with different cathode/anode ratios, $R = 2.0$, 2.5 and 3.0. All cells were charged at an approximate 0.7 C rate. The voltage and current profiles both show that the lower the carbon utilization in the anode (low R value), the better the quick-charge capability (shorter float time on charge). In this case, the P value increased from 1.44 (for $R = 2.0$), to 2.09 (for $R = 3.0$). Comparing the coke and graphite anodes, Figs. 7 and 8 show the corresponding coke anode version for Figs. 5 and 6. The current profiles in these figures were much smoother than those for graphite. The increase in P values with respect to charge rates and R values was not as significant in the coke cells as that in the graphite cells (Fig. 10). For a better visualization of the difference between coke and graphite anodes, Fig. 9 plots the voltage and current profiles at three different charge rates, C/4, C/2 and C for both graphite ($R = 2.5$) and coke ($R = 2.0$) anode cells. The voltage profiles for the graphite cells in this figure were shifted up by 1.5 V for clarity. It can be observed from this figure that the coke anode has a better quick-charge capability than that of the graphite anode. Fig. 10 quantifies the influence of cathode/anode ratios and charge rates on the P value for both coke and graphite anode cells. The P values in all cases increased as charge rates and cathode/anode ratios increased. Compared to graphite-anode cells, the P values in the coke-anode cells increased much less dramatically than those in the graphite

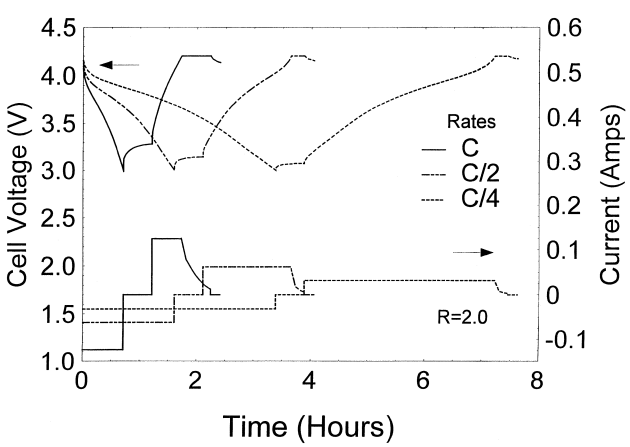

Fig. 7. Three voltage and current profiles collected on the second cycle from three coke cells in group C1. Each cell was discharged and charged at a different current rate ranging from C/4 to C. As charge rates increased, the current float times increased, but not as dramatically as in the graphite cells.

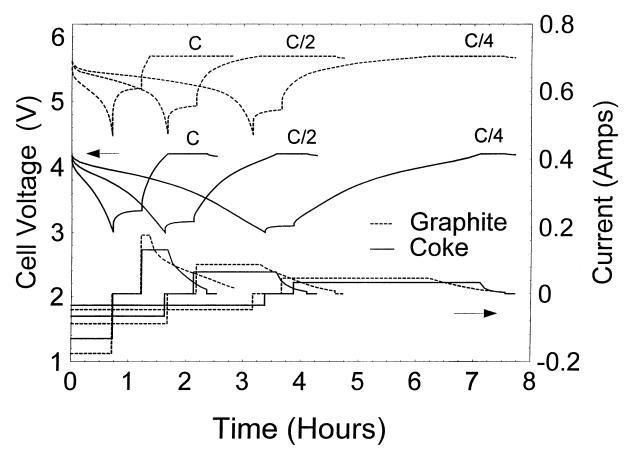

Fig. 9. Comparison of voltage and current profiles from three graphite cells (group G2) and three coke cells (group C1). All cells were charged and discharged at C/4 rate and data were collected on the second cycle. It can be seen that coke cells required less voltage float when compared to the graphite cell at the same charge rate.

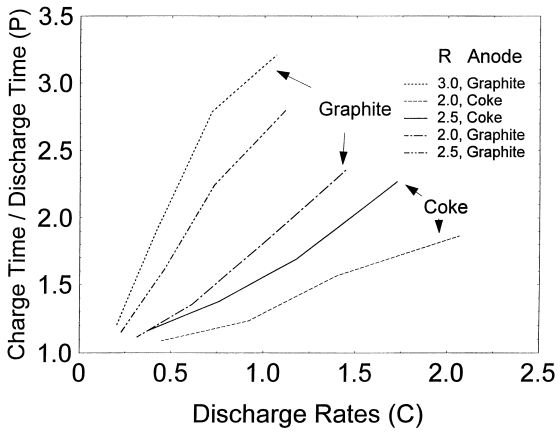

Fig. 10. Quantitative summary for the relation between cathode/anode ratios (R), charge rate and P values for graphite and coke cells. At the same lithium specific capacity for the graphite anode and the coke anode for cell groups G1 and C2, the coke anode cell outperformed the graphite cells.

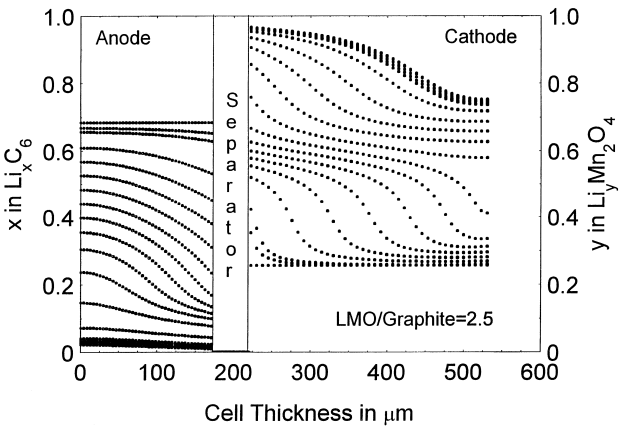

Fig. 11. Simulation for the lithium distribution over the anode and LMO cathode during cell discharge at 1 mA/cm^2. The lithium distribution remained relatively evenly distributed in the cell.

cells. This was true even when the graphite-anode cells utilized the same specific capacity as the coke-anode cells. The P value for the graphite cells in group G1 ($R = 2.0$) and the coke cells in group C2 ($R = 2.5$) is shown in Fig. 10 as a function of charge rate. These two cell groups utilized very similar specific carbon capacities (205 mA h/g). Even in this extreme case, coke cells still outperformed graphite cells with respect to the fast-charge capability. The superior quick-charge capability of coke cells likely benefited from both the coke's small carbon layers, for quick lithium access to active sites, and the coke's sloping and high lithium insertion voltage vs. lithium, producing a strong driving force for lithium insertion.

The difference between coke and graphite during rapid lithium insertion could be made clear if one would have a snapshot of lithium distribution in the anode during charging. Fortunately, a mathematical simulation model based on the concept of the Bellcore-type polymer lithium-ion cell has been developed by Newman and Doyle [10]. This model simulation has made it possible to evaluate lithium concentration distributions in the carbon anode during cell charge and discharge. The cell simulation model and its principals of operation have been detailed in Ref. [10]. The model parameters include the cell variables (porosity, anode and cathode composition, electrode and separator thickness, initial lithium content in LMO and graphite, anode and cathode film resistances, etc.) and material properties (densities, theoretical specific capacities for graphite and LMO, diffusion coefficients of carbon and LMO, etc.). The same adjustable input parameters, such as diffusion coefficients for graphite and LMO, film resistance, etc., need to be finely tuned to fit the discharge and charge voltage curves for final simulation calculations. Figs. 11 and 12 show the simulated lithium concentration distributions over the graphite anode and LMO cathode during cell discharge at an approximate C/4 rate. The simulation was based upon a set of practical cell parameters and the matching of the cell discharge and charge voltage curves (not included in this paper). It was clear that during the entire cell discharge, the lithium was evenly distributed in both the graphite anode and the LMO cathode. However, during charging, the lithium distribution in the graphite anode became extremely uneven and excessive near the interface between anode and separator at the end of charge, although the lithium remained more evenly distributed in the LMO cathode. It is the slow insertion process in the graphite anode that makes the constant-voltage float during cell charging a necessity for relaxation of the lithium distribution in the anode returning the cell back to its full capacity. A similar simulation performed on the coke anode cell (Fig. 13) indicated that the lithium distribution over the entire coke anode and LMO cathode during cell charge was fairly smooth even at twice the normal charge rate. The lithium distribution in the coke anode during charge was, therefore, much smoother, up to C/2 when compared to graphite, as shown in Figs. 11 and

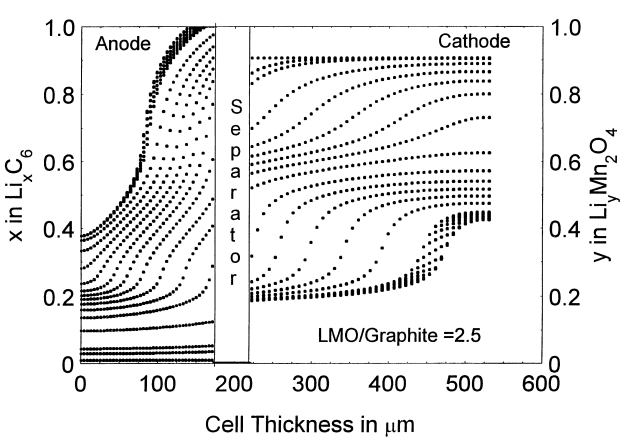

Fig. 12. Simulation for the lithium distribution over the graphite anode and LMO cathode during cell charge at 1 mA/cm^2. The lithium distribution is uneven in the anode during cell charge.

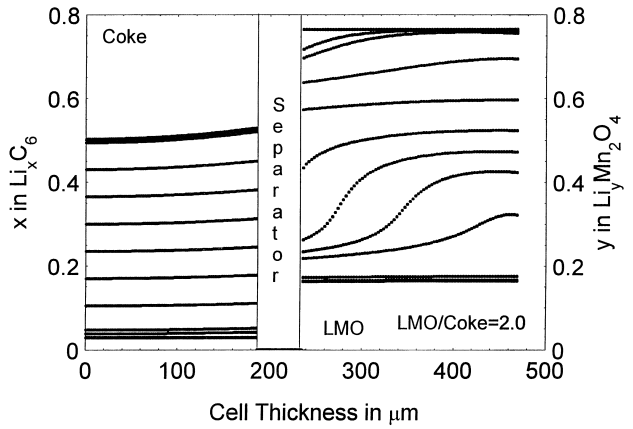

Fig. 13. Simulation for the lithium distribution over the coke anode and LMO cathode during cell charge at 1 mA/cm^2. The lithium distribution is evenly distributed in the coke anode during cell charge.

12. This result indicated that the lithium insertion process in the coke anode material was much faster than that occurring in the graphite anode. The simulation results were, therefore, consistent with the results from the inspection of cell voltage float char-acteristics.

Besides the cell charge rates and cathode/anode ratios (R), there are many other factors that could also influence the lithium insertion rate in the anode. Fig. 14 shows two charge current profiles for a graphite cell (G2 group) for the second and the 240th cycle, respectively, at an approximate C/4 rate. It can be seen that cell aging during life-cycling has a dramatic influence on the lithium insertion rate for the graphite anode. The P value for this case increased from 1.5 at the second cycle to 2.3 at the 240th cycle (an increase of 53%). The aging effect also occurred in the coke anode, but coke demonstrated a better resistance against aging during life-cycling when compared to

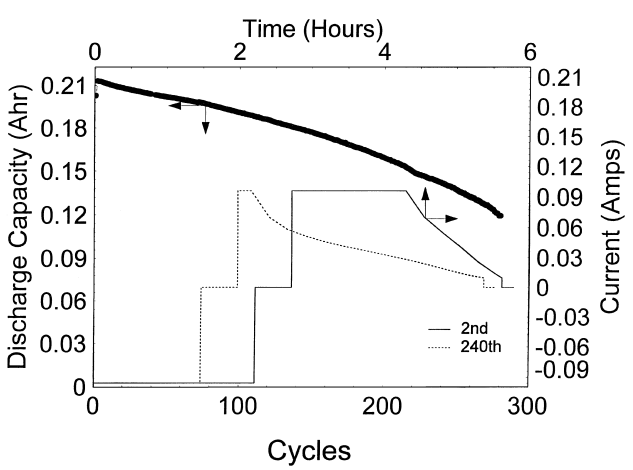

Fig. 14. Aging effect on the rate of lithium insertion in the graphite anode. The graphite cell from group G2 was cycled at a C/4 rate. The current profiles were collected on the second cycle and the 240th cycle. The P value increased considerably by 53% from 1.5 (2nd cycle) to 2.3 (240th cycle).

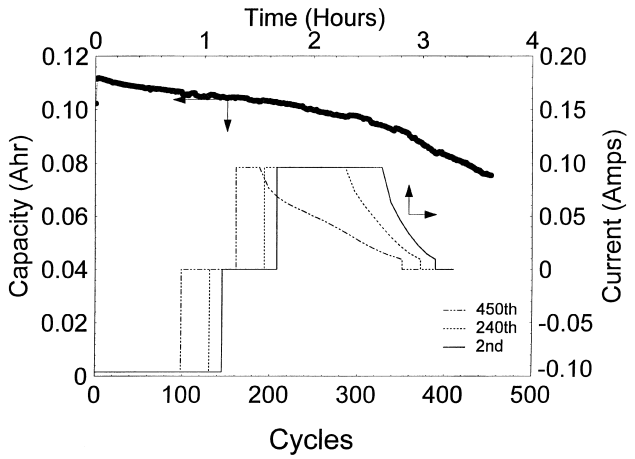

Fig. 15. Aging effect on the rate of lithium insertion in the coke anode. The coke cell from group G2 was cycled at a C/2 rate. The current profiles were collected on the second cycle, 240th cycle and 450th cycle. The P value increased by 9.6% from the 2nd cycle ($P = 1.25$) to the 240th cycle ($P = 1.37$), significantly less than that for graphite.

graphite. Fig. 15 shows the case for a coke anode cell during life-cycling at an approximately C rate. Three current profiles for various cycles, 2nd, 240th and 450th, are also shown in the figure. The P value increased from 1.25 (2nd cycle), to 1.37 (240th cycle) and then to 1.93 (450th cycle). From the second cycle to the 240th cycle, the P value increased by 9.6%. This is significantly less than the increase in the graphite anode cell over the same number of cycles (53%). Due to the disordered nature and smaller carbon layers of the coke material, lithium insertion caused much less volume expansion when compared to that for

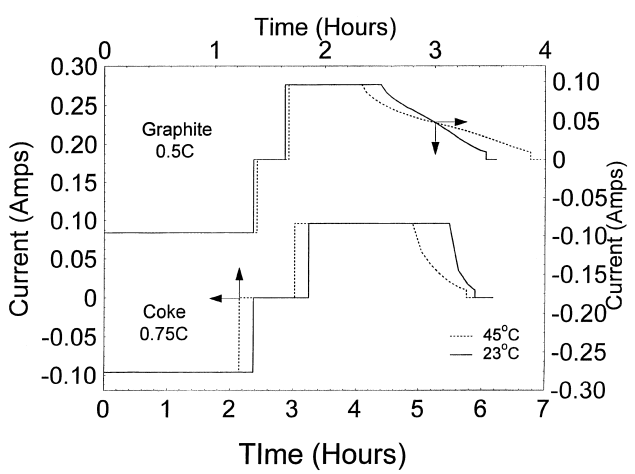

Fig. 16. Temperature effect on the rate of lithium insertion in carbon anodes. Two current profiles (2nd cycle) collected at two different temperatures (23°C and 45°C) are shown for the coke cell (group C1) and graphite cell (group G2), respectively. The coke and graphite cells were cycled at slightly different rates (0.75 C for the coke cell and 0.5 C for the graphite cell). It is clear that at the elevated temperature of 45°C, the rate of the lithium insertion in the anodes was much faster than that at 23°C. The P value decreased from 1.59 (23°C) to 1.35 (45°C) for the graphite anode cell and from 1.28 (23°C) to 1.12 (45°C) for the coke anode cell.

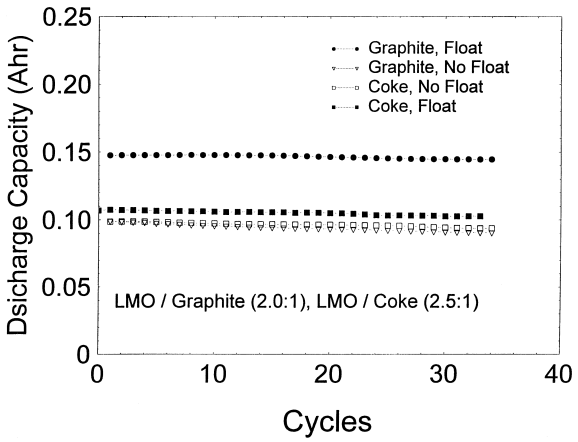

Fig. 17. Life cycle comparison between the coke cell (group C2) and the graphite cell (group G1). Both cells utilized the same specific capacity from either the coke or graphite material (205 mA h/g). Cells were cycled with and without voltage float during the charge for both cells. This figure shows the first 30 cycles of two graphite and two coke cells cycled with and without a charge voltage float. The graphite cell was cycled at 0.65 C and the coke cells at 1 C. The coke anode was much less affected after the removal of the voltage float than the graphite cell.

graphite (on order of 10%). This superior aging effect of the coke anode cell is most likely attributed to this reduced volume expansion in the coke anode during cell cycling. Another factor significantly influencing the lithium insertion rate is the temperature at which the cell is cycled. An example is given in Fig. 16. Second-cycle charge current profiles at two different temperatures (23°C and 45°C) are shown for the coke and graphite cells, respectively. The coke and graphite cells were cycled at slightly different rates, approximately 0.75 C and 0.5 C, respectively. The cells cycled at the elevated temperature (45°C) clearly showed higher rates of lithium insertion in the anode, which is indicated by the shorter float times. The P value was reduced from 1.59 at 23°C to 1.35 at 45°C for the graphite-anode cell (an 18% decrease), and from 1.28 at 23°C to 1.12 at 45°C for the coke-anode cell (a 15% decrease).

It has been demonstrated that there are several factors which influence the rate of lithium insertion in coke and graphite anodes. Due to the slow lithium insertion process during quick-cell charge, it is normally necessary to use a current float in order to fully charge the cell. The increase in charge time from using a current float depends considerably on the cell construction and carbon anode selection. It would be ideal to eliminate the current float altogether in order to save charge time without influencing the charge capacity. Normally, for graphite anode cells, removing the current float will reduce the charge capacity to as little as 50–75% of the discharge capacity depending on the cell construction and charge rate. For the coke anode cells, however, the current float has a much lower impact on charge capacity when compared to that for graphite. To compare the effect of the removal of current float on charge capacity between coke and graphite anodes, two graphite cells from group G1 and two coke cells from group C2 were cycled with and without current float at room temperature, respectively. As previously stated, the cathode/anode ratios for these two cell groups were selected so that the two groups had almost identical carbon utilizations (205 mA h/g) in the anode, and therefore, the comparison can be shifted to the nature of carbons. Fig. 17 shows the first 30 cycles for these four cells. The graphite cell was cycled at approximately 0.65 C and the coke cells at the 1 C rate. Clearly, the coke anode was much less affected by the removal of the voltage float when compared to the graphite cell with the same carbon anode utilization.

4. Conclusions

The graphite material showed a higher reversible lithium capacity and flatter lithium insertion voltage profile when compared to coke material. Both the crystallinity (large carbon layers) and low flat lithium insertion voltage for graphite create a slow rate material for lithium insertion. The lithium-ion cells using a graphite anode had a poor performance during quick-charge due to the slow lithium intercalation process occurring in the graphite anode. In contrast, the coke material had much smaller carbon layers and a sloping lithium insertion voltage profile. These properties significantly improve the rate of lithium insertion, and therefore, the cells using a coke anode showed a much better rate capability. It is believed that the coke material is structurally and electrochemically superior to graphite when used in high-rate applications. Both the experimental data and the computer simulation results are consistent with each other and support this conclusion.

Acknowledgements

The author wishes to thank Prof. J. Newman and Dr. M. Doyle for their kind assistance during the set-up and use of their simulation program. I also would like to thank Dr. R. Brodd for his consistent encouragement and many useful discussions throughout this work.

References

[1] Papers in the 8th International Meeting on Lithium Batteries, Nagoya, June 16–21, 1996.
[2] H. Shi et al., J. Electrochem. Soc. 143 (1996) 3466.
[3] A. Naji, J. Ghanbaja, P. Wilimann, D. Billaud, Carbon 35 (1997) 845.
[4] J. Dahn et al., Electrochim. Acta 38 (1993) 1179.

[5] B.D. Cullity, Elements of X-ray Diffraction, Addison Wesley Publishing.
[6] A.H. Thompson, J. Electrochem. Soc. 126 (1979) 608.
[7] Hang Shi, J. Remines, J.R. Dahn, J. Appl. Crystal, 26 (1993) 827–836.
[8] S. Atlung, B. Zachau-Christiansen, K. West, T. Jacobsen, J. Electrochem. Soc. 131 (1984) 1200.
[9] A.S. Gozdz, C.N. Schmutz, J.M. Tarascon, P.C. Warren, U.S. Patent 5,456,000, 1995.
[10] J. Newman, M. Doyle, J. Electrochem. Soc. 143 (1996) 1890.